MICROBURST SCALE SIZE DERIVED FROM MULTIPLE BOUNCES OF A MICROBURST SIMULTANEOUSLY OBSERVED WITH THE FIREBIRD-II CUBESATS

Contribution of Authors and Co-Authors

Manuscript(s) in Chapter(s) 1

Author: [type author name here]

Contributions: [list contributions here, single-spaced]

Co-Author: [type co-author name here]

Contributions: [list contributions here, single-spaced]

Co-Author: [type co-author name here]

Contributions: [list contributions here, single-spaced]

14 Manuscript Information

15 [Type Author and Co-author(s) Names Here]

16 Geophysical Research Letters

17 Status of Manuscript: Published in a peer-reviewed journal

18 Wiley

19 Volume 45, Issue 17

Key Points

- Multiple bounces from a microburst were observed by the two FIREBIRD-II CubeSats at LEO.
- The lower bounds on the microburst scale size at LEO were 29 ± 1 km (latitudinal) and 51 ± 11 km (longitudinal).
- Deduced lower bound equatorial scale size was similar to the whistler-mode chorus source scale.

ABSTRACT

We present the observation of a spatially large microburst with multiple bounces made simultaneously by the FIREBIRD-II CubeSats on February 2nd, 2015. This is the first observation of a microburst with a subsequent decay made by two co-orbiting but spatially separated spacecraft. From these unique measurements, we place estimates on the lower bounds of the spatial scales as well as quantify the electron bounce periods. The microburst's lower bound latitudinal scale size was 29 ± 1 km and the longitudinal scale size was 51 ± 1 km in low earth orbit. We mapped these scale sizes to the magnetic equator and found that the radial and azimuthal scale sizes were at least 500 ± 10 km and 530 ± 10 km, respectively. These lower bound equatorial scale sizes are similar to whistler-mode chorus wave source scale sizes, which supports the hypothesis that microbursts are a product of electron scattering by chorus waves. Lastly, we estimated the bounce periods for 200-800 keV electrons and found good agreement with four common magnetic field models.

Introduction

The dynamics of radiation belt electrons are complex, and are driven by competition between source and loss processes. A few possible loss processes are radial diffusion (Shprits and Thorne, 2004), magnetopause shadowing (Ukhorskiy et al., 2006), and pitch angle and energy diffusion due to scattering of electrons by plasma waves (e.g. Abel and Thorne, 1998; Horne and Thorne, 2003; Meredith et al., 2002; Mozer et al., 2018; Selesnick et al., 2003; Summers et al., 1998; Thorne et al., 2005). There are a variety of waves that cause pitch angle scattering, including electromagnetic ion cyclotron waves, plasmaspheric hiss, and chorus (Millan and Thorne, 2007; Thorne, 2010). Chorus predominantly occurs in the dawn sector (6-12 magnetic local times (MLT)) (Li et al., 2009) where it accelerates electrons with large equatorial pitch angles and scatters electrons with small equatorial pitch angles (Horne and Thorne, 2003). Some of these electrons may be impulsively scattered into the loss cone, where they result in short-duration ($\sim$ 100 ms) enhancements in precipitating flux called microbursts.

Anderson and Milton (1964) coined the term microburst to describe high altitude balloon observations of $\sim$ 100 ms duration enhancements of bremsstrahlung X-rays emitted from scattered microburst electrons impacting the atmosphere. Since then, non-relativistic (less than a few hundred keV) microbursts have been routinely observed with other balloon missions (e.g. Anderson et al., 2017; Parks, 1967; Woodger et al., 2015). A review of the literature shows no reports of microbursts above a few hundred keV observed by balloons (Millan et al., 2002; Woodger et al., 2015). This lack of observation may be explained by relatively weaker pitch angle scattering of

relativistic electrons by chorus (Lee et al., 2012).

In addition to the X-ray signature for bursts of electron precipitation, the precipitating relativistic and non-relativistic electrons have been measured in situ by spacecraft orbiting in low earth orbit (LEO). Hereinafter, we refer to these electron signatures observed by LEO spacecraft also as microbursts. Microbursts have been observed with, e.g. the Solar Anomalous and Magnetospheric Particle Explorer's (SAMPEX) ¿ 150 keV and ¿ 1 MeV channels (Blake et al., 1996; Blum et al., 2015; Lorentzen et al., 2001a,b; Nakamura et al., 1995, 2000; O'Brien et al., 2004, 2003) and Focused Investigation of Relativistic Electron Bursts: Intensity, Range, and Dynamics (FIREBIRD-II) with its ¿ 200 keV energy channels (Anderson et al., 2017; Breneman et al., 2017; Crew et al., 2016).

Understanding microburst precipitation and its scattering mechanism is important to radiation belt dynamics. The scattering mechanism has been observationally studied by e.g. Lorentzen et al. (2001b) who found that microbursts and chorus waves predominantly occur in the dawn sector and Breneman et al. (2017) made a direct observational link between individual microbursts and chorus elements. Microbursts have been modeled and empirically estimated to be capable of depleting the relativistic electron population in the outer radiation belt on the order of a day (Breneman et al., 2017; O'Brien et al., 2004; Shprits et al., 2007; Thorne et al., 2005). An important parameter in this estimation of instantaneous radiation belt electron losses due to microbursts is their scale size. Parks (1967) used balloon measurements of bremsstrahlung X-rays to estimate the high altitude scale size of predominantly low energy microbursts to be 40 ± 14 km. In Blake et al. (1996) a microburst with multiple bounces was observed by SAMPEX, and the microburst's latitudinal scale size in LEO was estimated to have been "at least a few tens of kilometers". Blake et al. (1996) concluded that typically microbursts are less than a few tens of electron gyroradii in

size (at L = 5 at LEO, the gyroradii of 1 MeV electrons is on the order of 100 m). Dietrich et al. (2010) used SAMPEX along with ground-based very low frequency stations to conclude that during one SAMPEX pass, the observed microbursts had scale sizes less than 4 km.

Since February 1st, 2015, microbursts have been observed by FIREBIRD-II, a pair of CubeSats in LEO. Soon after launch, when the two FIREBIRD-II spacecraft were at close range, a microburst with a scale size greater than 11 km was observed (Crew et al., 2016). On the same day, FIREBIRD-II simultaneously observed a microburst with multiple bounces. The microburst decay was observed over a period of a few seconds, while the spacecraft were traveling predominantly in latitude. Here we present the analysis and results of the latitude and longitude scale sizes and bounce periods of the first microburst with multiple bounces observed with the two FIREBIRD-II spacecraft.

Spacecraft and Observation

The FIREBIRD missions are comprised of a pair of identically-instrumented 1.5U CubeSats (15 x 10 x 10 cm) that are designed to measure electron precipitation in LEO (Klumpar et al., 2015; Spence et al., 2012). The second mission, termed FIREBIRD-II, was launched on January 31st 2015. The two FIREBIRD-II CubeSats, identified as Flight Unit 3 (FU3) and Flight Unit 4 (FU4), were placed in a 632 km apogee, 433 km perigee, and 99° inclination orbit (Crew et al., 2016). FU3 and FU4 are orbiting in a string of pearls configuration with FU4 ahead, to resolve the space-time ambiguity of microbursts. Each FIREBIRD-II unit has two solid state detectors: one is mounted essentially at the spacecraft surface, covered only by a thin foil acting as a sun shade, with a field of view of 90° (surface detector), and the other is beneath a collimator which restricts the field of view to 54° (collimated detector). Only FU3

has a functioning surface detector, so this analysis utilizes the collimated detectors. FU3's surface and collimated detectors, as well as FU4's collimated detector observe electron fluxes in six energy channels from $\sim$ 230 keV to $>$ 1 MeV. FIREBIRD-II's High Resolution (HiRes) electron flux data is gathered with an adjustable sampling period of 18.75 ms by default and can be as fast as 12.5 ms.

On February 2nd, 2015 at 06:12 UT, both FIREBIRD-II spacecraft simultaneously observed an initial microburst, followed by subsequent periodic electron enhancements of diminishing amplitude shown in Fig. 1.1. This is thought to be the signature of a single burst of electrons, some of which precipitate, but the rest mirror near the spacecraft then bounce to the conjugate hemisphere where they mirror again and the subsequent bounces produce a train of decaying peaks (Blake et al., 1996; Thorne et al., 2005). This bounce signature occurred during the transition between the main and recovery phases of a storm with a minimum Dst of -44 nT (Kp = 4, and AE $\approx$ 400 nT). At this time, the HiRes data was sampled at 18.75 ms. Five peaks were observed by both spacecraft. The fifth peak observed by FU4 was comparable to the Poisson noise and was not used in this analysis. This microburst was observed from the first energy channel ($\approx 200 - 300$ keV), to the fourth energy channel ($\approx 500 - 700$ keV), and FU3's surface detector observed the microburst up to the fifth energy channel (683 - 950 keV).

The HiRes data in Fig. 1.1 shows signs of energy dispersion, characterized by higher energy electrons arriving earlier than the lower energies. This time of flight energy dispersion tends to smear out the initial sharp burst upon each subsequent bounce. The first peak does not appear to be dispersed, and subsequent peaks show a dispersion trend consistent across energy channels. The black vertical bars have been added to Fig. 1.1 to highlight this energy dispersion. This dispersion signature and amplitude decay implies that the first peak was observed soon after the electrons

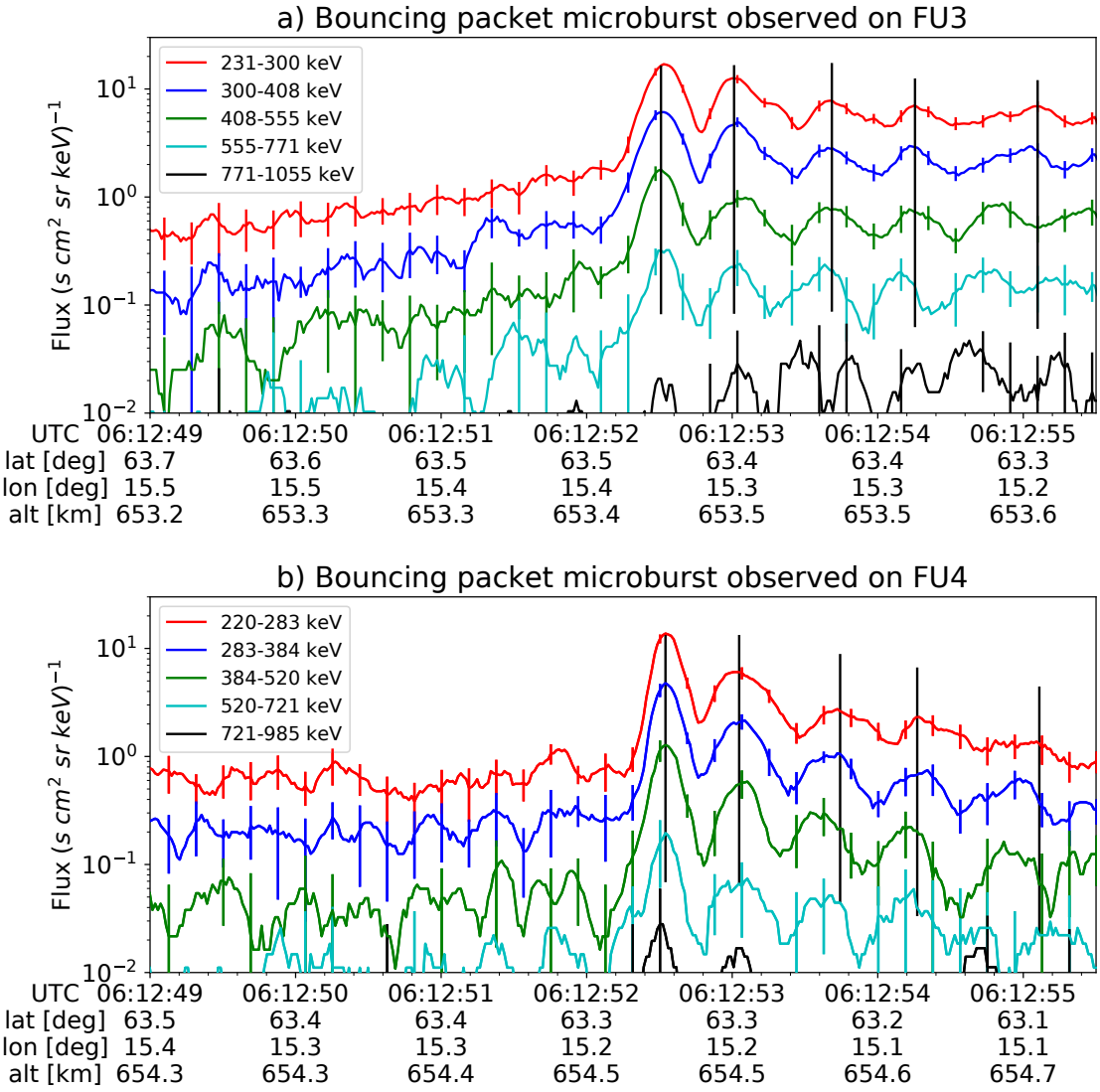

Figure 1.1: HiRes data of the microburst observed at February 2nd, 2015 at 06:12:53 UT, smoothed with a 150 ms rolling average. The subsequent bounces showed some energy dispersion. As discussed in Appendix A, a time correction of -2.28 s was applied to FU3. While the flux from five energy channels is shown, only channels with reasonable counting statistics were used for the spatial scale analysis. Vertical colored bars show the $\sqrt{N}$ error every 10th data point and vertical black bars are lined up with the peaks in the 220-283 keV energy channel to help identify dispersion.

were scattered, followed by decaying bounces.

At this time, in magnetic coordinates, FIREBIRD-II was at McIlwain L = 4.7 and MLT = 8.3, calculated with the Tsyganenko 1989 (T89) magnetic field model (Tsyganenko, 1989) using IRBEM-Lib (Boscher et al., 2012). Geographically, they were above Sweden, latitude = 63°N, longitude = 15°E, altitude = 650 km. This geographic location is magnetically conjugate to the east of the so-called South Atlantic Anomaly (SAA). The SAA is the location where the mirror points of electrons tend to occur at locations deeper in the atmosphere owing to the offset of the dipole magnetic field from the Earth's center. Electrons with pitch angles within the drift loss cone (DLC) will encounter the SAA and be removed from their eastward longitudinal drift paths (Comess et al., 2013; Dietrich et al., 2010). FU3 and FU4 are therefore both in regions where the particles in the DLC have recently precipitated, leaving only particles that were recently scattered. At the spacecraft location, locally mirroring electrons would have mirrored at 95 km in the opposite hemisphere, with more field aligned electrons mirroring at even lower altitudes. From the analysis done by Fang et al. (2010), the peak in the total ionization rate in the atmosphere for 100 keV electrons is around 80 km altitude, while the total ionization rate from 1 MeV electrons peaks around 60 km altitude. It is, therefore, expected that a fraction of the microburst electrons will survive each encounter with the atmosphere. By plotting the peak flux as a function of bounce (not shown), it was found that 40 - 60 % of the microburst electrons were lost on the first bounce, similar to the 33% loss per bounce observed for a bouncing microburst observed by SAMPEX (Thorne et al., 2005).

Analysis

At the beginning of the FIREBIRD-II mission, two issues prevented the proper analysis of the microburst's spatial scale size: the spacecraft clocks were not

synchronized, and their relative positions were not accurately known. We addressed these issues with a cross-correlation time lag analysis described in detail in Appendix A. From this analysis, the time correction was 2.28 ± 0.12 s (applied to Fig. 1.1) and the separation was 19.9 ± 0.9 km at the time of the microburst observation.

Electron Bounce Period

We used this unique observation of bouncing electrons to calculate the bounce period, t_b as a function of energy and compare it to the energy-dependent t_b curves derived from four magnetic field models, the results of which are shown in Fig. 1.2. The observed t_b and uncertainties were calculated by fitting the baseline-subtracted HiRes flux. The baseline flux used in this analysis is given in O'Brien et al. (2004) as the flux at the 10th percentile over a specified time interval, which in this analysis was taken to be 0.5 seconds. The flux was fitted with a superposition of Gaussians for each energy channel, and the uncertainty in flux was calculated using the Poisson error from the microburst and baseline fluxes summed in quadrature. Using the fit parameters, the mean t_b for the lowest four energy channels is shown in Fig. 1.2. The trend of decreasing t_b as a function of energy is evident in Fig. 1.2, which further supports the assumption that the subsequent peaks are bounces, and not a train of microbursts scattered by bouncing chorus.

The decaying peaks in the 231-408 keV electron flux observed by FU3's lowest two energy channels (see Fig. 1.1) were right-skewed. One explanation is that there was in-channel energy dispersion within those channels. Since t_b of higher energy electrons is shorter, a right-skewed peak implies that higher energy electrons were more abundant within that channel e.g. in FU3's 231-300 keV channel, the 300 keV electrons will arrive sooner than the 231 keV electrons, but will they will be binned in the same channel. A Gaussian fit cannot account for this in-channel dispersion,

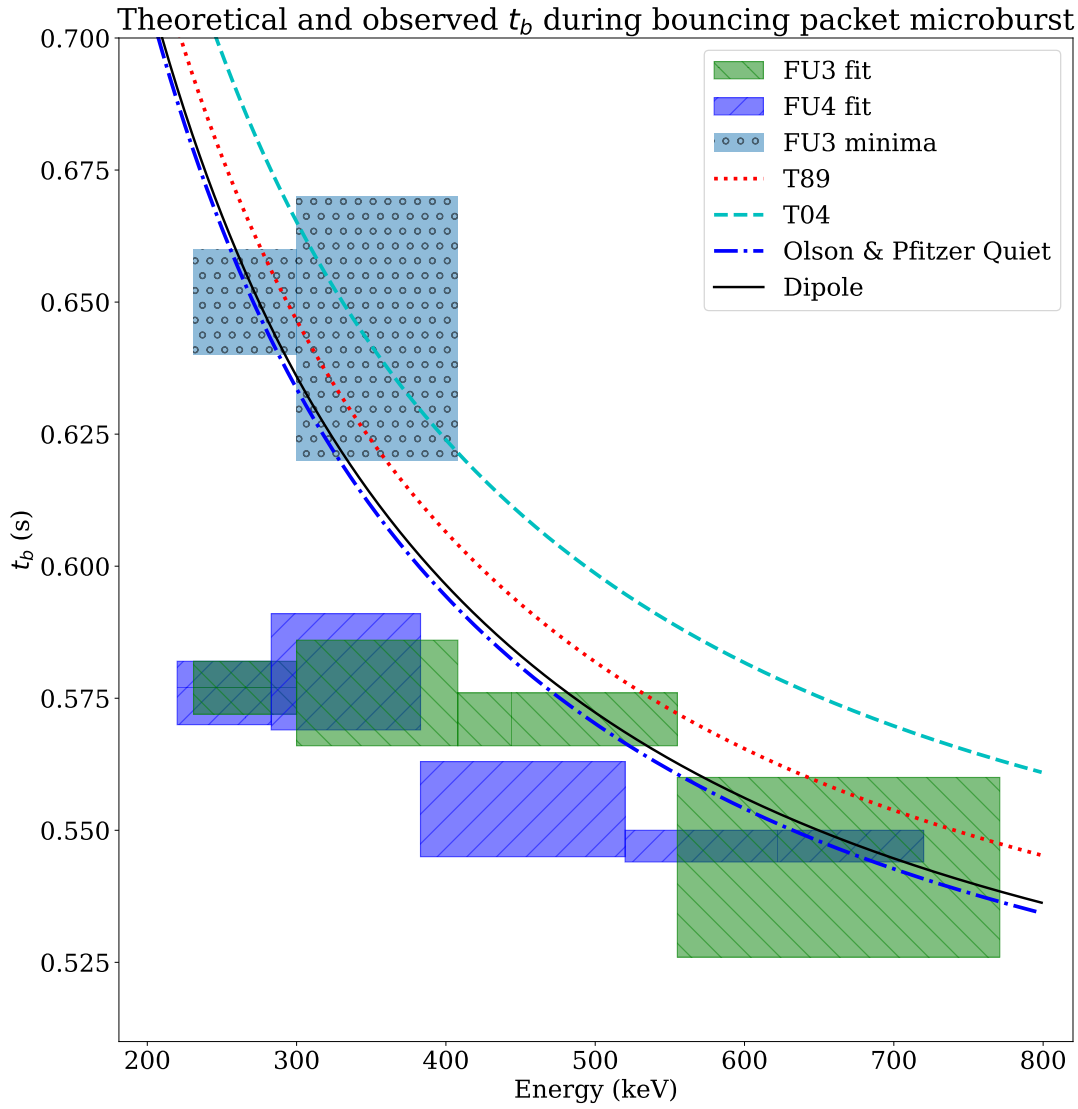

Figure 1.2: Observed and theoretical t_b for electrons of energies from 200 to 770 keV. The solid black line is t_b in a dipole magnetic field, derived in Schulz and Lanzerotti (1974). The red dotted and cyan dashed lines are the t_b derived using the T89, and T04 magnetic field models with IRBEM-Lib. Lastly, the blue dot-dash curve is the t_b derived using the Olson & Pfitzer Quiet model. The green and purple rectangles represent the observed t_b for FU3 and FU4 using a Gaussian fit, respectively. The blue rectangles represent the observed t_b calculated with the minima between the bounces. The width of the boxes represent the width of those energy channels, and the height represents the uncertainty from the fit.

and as a first order correction, minima between peaks was used to calculate t_b, and is shown in Fig. 1.2. The observed energy-dependent dispersion shown in Fig. 1.2 is consistent with higher energy peaks returning sooner. This dispersion consistency further supports the assumption that the subsequent peaks are bounces, and not a train of microbursts scattered by bouncing chorus.

To compare the observed and modeled t_b, we superposed t_b curves for various models including an analytical solution in a dipole (Schulz and Lanzerotti, 1974), and numerical models: T89, Tsyganenko 2004 (T04) (Tsyganenko and Sitnov, 2005), and Olson & Pfitzer Quiet (Olson and Pfitzer, 1982) in Fig. 1.2. The numerical t_b curves were calculated using a wrapper for IRBEM-Lib. This code traces the magnetic field line between mirror points, and calculates t_b assuming conservation of energy and the first adiabatic invariant for electrons mirroring at FIREBIRD-II. With the empirical t_b, the models agree within FIREBIRD-II's uncertainties, but the T04 model has the largest discrepancy compared to the other models.

Microburst Energy Spectra

Next, we investigated the energy spectra of this microburst. The energy spectra was modeled with an exponential that was fit to the peak flux derived from the Gaussian fit parameters in section 1 to all but the highest energy channel. We found that the E-folding energy, $E_0 \sim 100$ keV. This spectra is similar to spectra show by Lee et al. (2005) from STSAT-1 and Datta et al. (1997) from sounding rocket measurements. The energy spectra is soft for a typical microburst observed with FIREBIRD-II and there was no statistically significant change in E_0 for subsequent bounces.

Microburst Scale Sizes

Lastly, after we applied the time and separation corrections detailed in Appendix A, we mapped the locations of FU3 and FU4 in Fig. 1.3. The locations where FU3 saw peaks 1-5 and where FU4 saw peaks 1-4 are shown as P1-5 and P1-4, respectively. The lower bound on the latitudinal extent of the microburst was the difference in latitude between P1 on FU3 and P4 on FU4 and was found to be 29 ± 1 km. The uncertainty was estimated from the spacecraft separation uncertainty described in Appendix A. This scale size is the largest reported by FIREBIRD-II.

In section 1, we showed that the observed decaying peaks were likely due to bouncing, so we assume that the observed electrons in subsequent bounces were the drifted electrons from the initial microburst. Under this assumption, the scattered electrons observed in the last bounce by FIREBIRD-II, must have drifted east from their initial scattering longitude, allowing us to calculate the minimum longitudinal scale size. Following geometrical arguments, the distance that electrons drift east in a single bounce is a product of the circumference of the drift shell foot print, and the fraction of the total drift orbit traversed in a single bounce and is given by,

$$d_{az} = 2\pi(R_E + A)\cos(\lambda)\frac{t_b}{\langle T_d \rangle} \tag{1.1}$$

where R_E is the Earth's radius, A is the spacecraft altitude, λ is the magnetic latitude, t_b is the electron bounce period, and $\langle T_d \rangle$ is the electron drift period. Parks (2003) derived $\langle T_d \rangle$ to be,

$$\langle T_d \rangle \approx \begin{cases} 43.8/(L \cdot E) & \text{if } \alpha_0 = 90^\circ \\ 62.7/(L \cdot E) & \text{if } \alpha_0 = 0^\circ \end{cases} \tag{1.2}$$

where E is the electron energy in MeV, L is the L shell, and α_0 is the equatorial pitch angle. Electrons mirroring at FIREBIRD-II have $\alpha_0 \approx 3.7^\circ$ and so the $\alpha_0 = 0^\circ$ limit

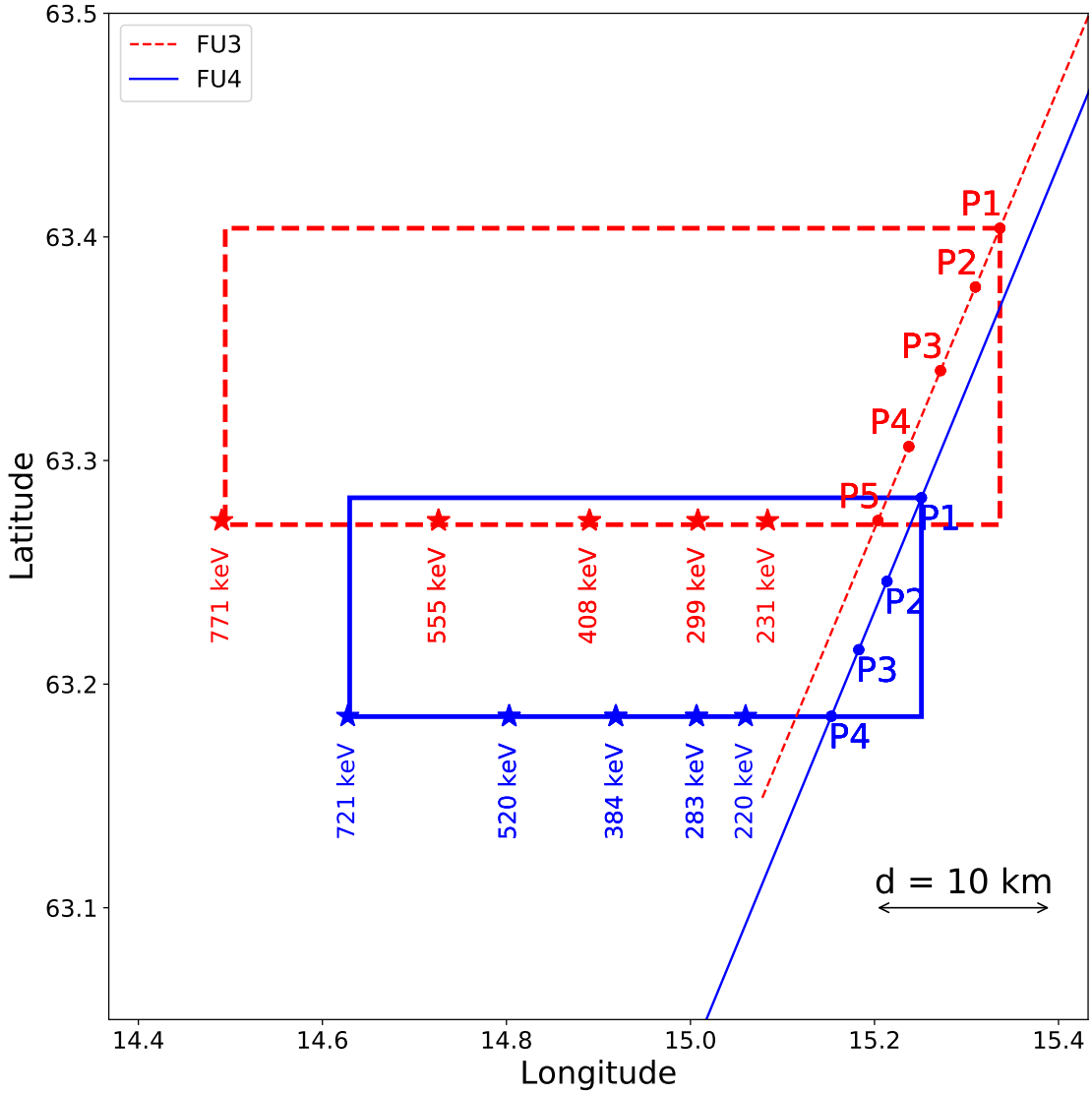

Figure 1.3: The topology of the FIREBIRD-II orbit and the multiple bounces of the microburst projected onto latitude and longitude with axis scaled to equal distance. Attributes relating to FU3 shown in red dashed lines, and FU4 with blue solid lines. The spacecraft path is shown with the diagonal lines, starting at the upper right corner. The labels P1-4 for FU4 and P1-5 for FU3 indicate where the spacecraft were when the N^{th} peak was seen in the lowest energy channel in the HiRes data. The stars with the accompanying energy labels represent the locations of the electrons with that energy that started at time of P1, and were seen at the last peak on each spacecraft. The rectangles represent the lower bound of the microburst scale size, assuming that the majority of the electrons were in the upper boundary of energy channel 4.

was used.

The microburst's longitudinal scale size is defined as the distance the highest energy electrons drifted in the time between the observations of the first and last peaks. This scale size is given by $D_{az} = n\ d_{az}$ where n is the number of bounces observed. The stars in Fig. 1.3 (with labels corresponding to energy channel boundaries) represent the locations when the microburst was observed at P1, such that an electron of that energy would drift eastward to be seen at P5 for FU3 and P4 for FU4. Since FU3 observed more peaks it observed the larger longitudinal scale size which is shown with the red dashed box in Fig. 1.3. FU3's fourth energy channel's bounds are 555 keV and 771 keV, which correspond to longitudinal distances of 39 ± 1 km and 51 ± 1, respectively. The uncertainty was estimated by propagating the uncertainty in the bounce time Eq. 1.1. While the observed minimum longitudinal scale size is dependent on FIREBIRD-II's energy channels, the true scale size may not be.

To investigate how the microburst scale size compares to the scale sizes of chorus waves near the magnetic equator, the microburst's longitudinal and latitudinal scale sizes and their uncertainties in LEO were mapped to the magnetic equator with T89. The radial scale size (latitudinal scale mapped from LEO) was greater than 500 ± 10 km. The azimuthal scale size (longitudinal scale mapped from LEO) of 555 keV electrons was greater than 450 ± 10 km and for the 771 keV electrons it was greater than 530 ± 10 km. The lower bound microburst scale size is similar to the chorus scale sizes derived by Agapitov et al. (2017, 2011), and is discussed below.

Discussion and Conclusions

We presented the first observation of a large microburst with multiple bounces made possible by the twin FIREBIRD-II CubeSats. The microburst's lower bound

LEO latitudinal and longitudinal scale sizes of 29 ± 1 km and 51 ± 1 km make it one of the largest observed. The microburst's LEO scale size was larger than the latitudinal scale sizes of typical ¿ 1 MeV microbursts reported in Blake et al. (1996), approximately 10 times larger than reported in Dietrich et al. (2010), and approximately 2.6 times larger than other simultaneous microbursts observed by FIREBIRD-II (Crew et al., 2016). Lastly, the scale sizes derived here were similar to the scale sizes of ¿ 15 keV microbursts observed with a high altitude balloon (Parks, 1967). No energy dependence on the minimum latitudinal scale size was observed, while the observed energy dependence of the minimum longitudinal scale size is an artifact of the technique we used to estimate their drift motion.

The microburst scale size obtained in Section 1 and scaled to the geomagnetic equator can be compared with the scales of chorus waves presumably responsible for the rapid burst electron precipitation. Early direct estimates of the chorus source scales were made by the coordinated measurement by ISEE-1, 2. The wave power correlation scale was estimated to be about several hundred kilometers across the background magnetic field (Gurnett et al., 1979). Furthermore, Santolik et al. (2003) determined the correlation lengths of chorus-type whistler waves to be around 100 km based on multipoint CLUSTER Wide Band Data measurements near the chorus source region at $L \approx 4$, during the magnetic storm of 18 April 2002. Agapitov et al. (2017, 2011, 2010) recently showed that the spatial extent of chorus source region can be larger, ranging from 600 km in the outer radiation belt to more than 1000 km in the outer magnetosphere. The lower bound azimuthal and latitudinal scales obtained in Section 1 and scaled to the magnetic equator, are similar to the whistler-mode chorus source scale sizes reported in Agapitov et al. (2017, 2011).

No wave measurements from nearby spacecraft were available at this time. Nevertheless, during the hours before and after this observation, the Van Allen Probes'

(Mauk et al., 2013) Electric and Magnetic Field Instrument and Integrated Science (Kletzing et al., 2013) observed strong wave power in the lower band chorus frequency range, inside the outer radiation belt between 22 and 2 MLT. Furthermore, AE $\sim$ 400 nT at this time, and relatively strong chorus waves were statistically more likely to be present at FIREBIRD-II's MLT (Li et al., 2009).

The empirically estimated and modeled t_b in this study agree within FIREBIRD-II's uncertainties, confirming that the energy-dependent dispersion was due to bouncing. The t_b curves are a proxy for field line length, and this agreement implies that they are comparable. This is expected since the magnetosphere is not drastically compressed at 8 MLT, but we expect a larger discrepancy near midnight, where the magnetosphere is more stretched and difficult to accurately model. In future studies, this analysis can be used as a diagnostic tool to validate field line lengths, and improve magnetic field models.

The similarity of the microburst and chorus source region scale sizes, as well as magnetospheric location and conditions, further support the causal relationship between microbursts and chorus.

Acknowledgments

This work was made possible with help from the FIREBIRD team, and the members of the Space Sciences and Engineering Laboratory at Montana State University for their hard work to make this mission a success. In addition, M. Shumko acknowledges Drew Turner for his suggestions regarding the bounce period calculations, and Dana Longcope for his proofreading feedback. The FIREBIRD-II data are available at http://solar.physics.montana.edu/FIREBIRD_II/. This analysis is supported by the National Science Foundation under Grant Numbers 0838034 and 1339414. Furthermore, the work of O. Agapitov was supported by the NASA grant

307 NNX16AF85G.

Bibliography

Abel, B. and Thorne, R. M. (1998). Electron scattering loss in earth's inner magnetosphere: 1. dominant physical processes. *Journal of Geophysical Research: Space Physics*, 103(A2):2385–2396.

Agapitov, O., Blum, L. W., Mozer, F. S., Bonnell, J. W., and Wygant, J. (2017). Chorus whistler wave source scales as determined from multipoint van allen probe measurements. *Geophysical Research Letters*, pages n/a–n/a. 2017GL072701.

Agapitov, O., Krasnoselskikh, V., Dudok de Wit, T., Khotyaintsev, Y., Pickett, J. S., Santolik, O., and Rolland, G. (2011). Multispacecraft observations of chorus emissions as a tool for the plasma density fluctuations' remote sensing. *Journal of Geophysical Research: Space Physics*, 116(A9):n/a–n/a. A09222.

Agapitov, O., Krasnoselskikh, V., Zaliznyak, Y., Angelopoulos, V., Le Contel, O., and Rolland, G. (2010). Chorus source region localization in the earth's outer magnetosphere using themis measurements. *Annales Geophysicae*, 28(6):1377–1386.

Anderson, B., Shekhar, S., Millan, R., Crew, A., Spence, H., Klumpar, D., Blake, J., O'Brien, T., and Turner, D. (2017). Spatial scale and duration of one microburst region on 13 August 2015. *Journal of Geophysical Research: Space Physics*.

Anderson, K. A. and Milton, D. W. (1964). Balloon observations of X rays in the auroral zone: 3. High time resolution studies. *Journal of Geophysical Research*, 69(21):4457–4479.

Blake, J., Looper, M., Baker, D., Nakamura, R., Klecker, B., and Hovestadt, D. (1996). New high temporal and spatial resolution measurements by sampex of the precipitation of relativistic electrons. *Advances in Space Research*, 18(8):171 – 186.

Blum, L., Li, X., and Denton, M. (2015). Rapid MeV electron precipitation as observed by SAMPEX/HILT during high-speed stream-driven storms. *Journal of Geophysical Research: Space Physics*, 120(5):3783–3794. 2014JA020633.

Boscher, D., Bourdarie, S., O'Brien, P., Guild, T., and Shumko, M. (2012). Irbem-lib library.

Breneman, A., Crew, A., Sample, J., Klumpar, D., Johnson, A., Agapitov, O., Shumko, M., Turner, D., Santolik, O., Wygant, J., et al. (2017). Observations directly linking relativistic electron microbursts to whistler mode chorus: Van allen probes and FIREBIRD II. *Geophysical Research Letters*.

Comess, M., Smith, D., Selesnick, R., Millan, R., and Sample, J. (2013). Duskside relativistic electron precipitation as measured by sampex: A statistical survey. *Journal of Geophysical Research: Space Physics*, 118(8):5050–5058.

Crew, A. B., Spence, H. E., Blake, J. B., Klumpar, D. M., Larsen, B. A., O'Brien, T. P., Driscoll, S., Handley, M., Legere, J., Longworth, S., Mashburn, K., Mosleh, E., Ryhajlo, N., Smith, S., Springer, L., and Widholm, M. (2016). First multipoint in situ observations of electron microbursts: Initial results from the NSF FIREBIRD II mission. *Journal of Geophysical Research: Space Physics*, 121(6):5272–5283. 2016JA022485.

Datta, S., Skoug, R., McCarthy, M., and Parks, G. (1997). Modeling of microburst electron precipitation using pitch angle diffusion theory. *Journal of Geophysical Research: Space Physics*, 102(A8):17325–17333.

Dietrich, S., Rodger, C. J., Clilverd, M. A., Bortnik, J., and Raita, T. (2010). Relativistic microburst storm characteristics: Combined satellite and ground-based observations. *Journal of Geophysical Research: Space Physics*, 115(A12).

Fang, X., Randall, C. E., Lummerzheim, D., Wang, W., Lu, G., Solomon, S. C., and Frahm, R. A. (2010). Parameterization of monoenergetic electron impact ionization. *Geophysical Research Letters*, 37(22).

Gurnett, D., Anderson, R., Scarf, F., Fredricks, R., and Smith, E. (1979). Initial results from the isee-1 and-2 plasma wave investigation. *Space Science Reviews*, 23(1):103–122.

Horne, R. B. and Thorne, R. M. (2003). Relativistic electron acceleration and precipitation during resonant interactions with whistler-mode chorus. *Geophysical Research Letters*, 30(10). 1527.

Kletzing, C., Kurth, W., Acuna, M., MacDowall, R., Torbert, R., Averkamp, T., Bodet, D., Bounds, S., Chutter, M., Connerney, J., et al. (2013). The electric and magnetic field instrument suite and integrated science (EMFISIS) on RBSP. *Space Science Reviews*, 179(1-4):127–181.

Klumpar, D., Springer, L., Mosleh, E., Mashburn, K., Berardinelli, S., Gunderson, A., Handly, M., Ryhajlo, N., Spence, H., Smith, S., Legere, J., Widholm, M., Longworth, S., Crew, A., Larsen, B., Blake, J., and Walmsley, N. (2015). Flight system technologies enabling the twin-cubesat firebird-ii scientific mission.

Lee, J. J., Parks, G. K., Lee, E., Tsurutani, B. T., Hwang, J., Cho, K. S., Kim, K.-H., Park, Y. D., Min, K. W., and McCarthy, M. P. (2012). Anisotropic pitch angle distribution of 100 keV microburst electrons in the loss cone: measurements from STSAT-1. *Annales Geophysicae*, 30(11):1567–1573.

Lee, J.-J., Parks, G. K., Min, K. W., Kim, H. J., Park, J., Hwang, J., McCarthy, M. P., Lee, E., Ryu, K. S., Lim, J. T., Sim, E. S., Lee, H. W., Kang, K. I., and Park, H. Y. (2005). Energy spectra of 170-360 keV electron microbursts measured by the korean STSAT-1. *Geophysical Research Letters*, 32(13). L13106.

Li, W., Thorne, R. M., Angelopoulos, V., Bortnik, J., Cully, C. M., Ni, B., LeContel, O., Roux, A., Auster, U., and Magnes, W. (2009). Global distribution of whistler-mode chorus waves observed on the THEMIS spacecraft. *Geophysical Research Letters*, 36(9). L09104.

Lorentzen, K. R., Blake, J. B., Inan, U. S., and Bortnik, J. (2001a). Observations of relativistic electron microbursts in association with VLF chorus. *Journal of Geophysical Research: Space Physics*, 106(A4):6017–6027.

Lorentzen, K. R., Looper, M. D., and Blake, J. B. (2001b). Relativistic electron microbursts during the GEM storms. *Geophysical Research Letters*, 28(13):2573–2576.

Mauk, B., Fox, N. J., Kanekal, S., Kessel, R., Sibeck, D., and Ukhorskiy, A. (2013). Science objectives and rationale for the radiation belt storm probes mission. *Space Science Reviews*, 179(1-4):3–27.

Meredith, N., Horne, R., Summers, D., Thorne, R., Iles, R., Heynderickx, D., and Anderson, R. (2002). Evidence for acceleration of outer zone electrons to relativistic energies by whistler mode chorus. In *Annales Geophysicae*, volume 20, pages 967–979.

Millan, R. and Thorne, R. (2007). Review of radiation belt relativistic electron losses. *Journal of Atmospheric and Solar-Terrestrial Physics*, 69(3):362 – 377.

Millan, R. M., Lin, R., Smith, D., Lorentzen, K., and McCarthy, M. (2002). X-ray observations of mev electron precipitation with a balloon-borne germanium spectrometer. *Geophysical research letters*, 29(24).

Mozer, F. S., Agapitov, O. V., Blake, J. B., and Vasko, I. Y. (2018). Simultaneous observations of lower band chorus emissions at the equator and microburst precipitating electrons in the ionosphere. *Geophysical Research Letters*.

Nakamura, R., Baker, D. N., Blake, J. B., Kanekal, S., Klecker, B., and Hovestadt, D. (1995). Relativistic electron precipitation enhancements near the outer edge of the radiation belt. *Geophysical Research Letters*, 22(9):1129–1132.

Nakamura, R., Isowa, M., Kamide, Y., Baker, D., Blake, J., and Looper, M. (2000). Observations of relativistic electron microbursts in association with VLF chorus. *J. Geophys. Res*, 105:15875–15885.

O'Brien, T. P., Looper, M. D., and Blake, J. B. (2004). Quantification of relativistic electron microburst losses during the GEM storms. *Geophysical Research Letters*, 31(4). L04802.

O'Brien, T. P., Lorentzen, K. R., Mann, I. R., Meredith, N. P., Blake, J. B., Fennell, J. F., Looper, M. D., Milling, D. K., and Anderson, R. R. (2003). Energization of relativistic electrons in the presence of ULF power and MeV microbursts: Evidence for dual ULF and VLF acceleration. *Journal of Geophysical Research: Space Physics*, 108(A8).

Olson, W. P. and Pfitzer, K. A. (1982). A dynamic model of the magnetospheric magnetic and electric fields for july 29, 1977. *Journal of Geophysical Research: Space Physics*, 87(A8):5943–5948.

Parks, G. (2003). *Physics Of Space Plasmas: An Introduction, Second Edition*. Westview Press.

Parks, G. K. (1967). Spatial characteristics of auroral-zone X-ray microbursts. *Journal of Geophysical Research*, 72(1):215–226.

Santolik, O., Gurnett, D., Pickett, J., Parrot, M., and Cornilleau-Wehrlin, N. (2003). Spatio-temporal structure of storm-time chorus. *Journal of Geophysical Research: Space Physics*, 108(A7).

Schulz, M. and Lanzerotti, L. J. (1974). *Particle Diffusion in the Radiation Belts*. Springer.

Selesnick, R. S., Blake, J. B., and Mewaldt, R. A. (2003). Atmospheric losses of radiation belt electrons. *Journal of Geophysical Research: Space Physics*, 108(A12). 1468.

Shprits, Y. Y., Meredith, N. P., and Thorne, R. M. (2007). Parameterization of radiation belt electron loss timescales due to interactions with chorus waves. *Geophysical Research Letters*, 34(11):n/a–n/a. L11110.

Shprits, Y. Y. and Thorne, R. M. (2004). Time dependent radial diffusion modeling of relativistic electrons with realistic loss rates. *Geophysical Research Letters*, 31(8):n/a–n/a. L08805.

Spence, H. E., Blake, J. B., Crew, A. B., Driscoll, S., Klumpar, D. M., Larsen, B. A., Legere, J., Longworth, S., Mosleh, E., O'Brien, T. P., Smith, S., Springer, L., and Widholm, M. (2012). Focusing on size and energy dependence of electron microbursts from the van allen radiation belts. *Space Weather*, 10(11).

Summers, D., Thorne, R. M., and Xiao, F. (1998). Relativistic theory of wave-particle resonant diffusion with application to electron acceleration in the magnetosphere. *Journal of Geophysical Research: Space Physics*, 103(A9):20487–20500.

Thorne, R. M. (2010). Radiation belt dynamics: The importance of wave-particle interactions. *Geophysical Research Letters*, 37(22). L22107.

Thorne, R. M., O'Brien, T. P., Shprits, Y. Y., Summers, D., and Horne, R. B. (2005). Timescale for MeV electron microburst loss during geomagnetic storms. *Journal of Geophysical Research: Space Physics*, 110(A9). A09202.

Tsyganenko, N. (1989). A solution of the chapman-ferraro problem for an ellipsoidal magnetopause. *Planetary and Space Science*, 37(9):1037 – 1046.

Tsyganenko, N. A. and Sitnov, M. I. (2005). Modeling the dynamics of the inner magnetosphere during strong geomagnetic storms. *Journal of Geophysical Research: Space Physics*, 110(A3).

Ukhorskiy, A. Y., Anderson, B. J., Brandt, P. C., and Tsyganenko, N. A. (2006). Storm time evolution of the outer radiation belt: Transport and losses. *Journal of Geophysical Research: Space Physics*, 111(A11):n/a–n/a. A11S03.

Woodger, L., Halford, A., Millan, R., McCarthy, M., Smith, D., Bowers, G., Sample, J., Anderson, B., and Liang, X. (2015). A summary of the BARREL campaigns: Technique for studying electron precipitation. *Journal of Geophysical Research: Space Physics*, 120(6):4922–4935.